# Characteristics and Application of Cascode GaN HEMT

En Fang[1,2](✉)

[1] School of Electrical and Control Engineering, Xuzhou University of Technology, Xuzhou 221018, Jiangsu, China
fangen@cumt.edu.cn
[2] Jiangsu Key Construction Laboratory of Large Engineering Equipment Testing and Control Technology, Xuzhou 221018, Jiangsu, China

**Abstract.** For the particular structure of cascode GaN HEMT, the parameters related to its output characteristics, transfer characteristics, driving characteristics, and switching characteristics are compared with Si MOSFETs under the same voltage and current level. And it is better than Si MOSFET. To obtain accurate switching loss and clarify the influence of various parameters on the switching process, a practical segmentation analysis model is established for the dynamic process of cascode GaN HEMT turn-on and turn-off, which is verified by the dual-pulse test hardware platform. The prediction of the process voltage and current waveform is accurate.

**Keywords:** Cascode · GaN device · Characteristics

## 1 Introduction

As the most important secondary energy in social production, electrical energy is widely used in the production and life of human society because of its clean, manageable control and easy transmission. Multiple transformations are needed in the process of power production, transmission, and consumption. As one of the critical technologies of power conversion, power electronic technology is more and more profoundly going into human life and affecting the progress of human civilization. After more than half a century of development, power electronics technology has been widely used in transportation, energy, national defense, and other fields of the national economy and people's livelihood. In today's world, energy shortage and environmental protection problems are becoming increasingly severe, and photovoltaic power generation, wind power generation and electric vehicle industry promote the continuous development of power electronic technology. At the same time, it also puts forward new requirements for power electronic devices and encourages them to develop in the direction of high frequency, high efficiency, and high power density.

After decades of development, the performance of Si-based power switching devices is approaching its material limits. The power electronic converter is limited to further


D. Jiang and H. Song (Eds.): SIMUtools 2021, LNICST 424, pp. 194–204, 2022.
https://doi.org/10.1007/978-3-030-97124-3_17

growth in the direction of high frequency, high efficiency, and high power density. As an outstanding representative of the third generation of wide bandgap semiconductor devices, Cascode GaN HEMT utilizes a cascode structure to achieve the normally-off nature of GaN devices, with unmatched steady-state and dynamic performance of Si-based devices. In order to promote its replacement of Si devices and give full play to the performance advantages of cascode GaN HEMTs, this thesis studies its characteristics and applications in hard switching and soft switching states.

## 2 Characteristics and Analysis of Cascode GaN HEMT

### 2.1 Performance Comparison

**Table 1.** List of device models.

| Current/A | Transphorm | Infineon | Fairchild | Vishay |
|---|---|---|---|---|
| 16 | TPH3206PSB | IPD65R250E6 | FCPF190N65 S3R0L | —— |
| 20 | TPH3208PS | IPP60R190C6 | FCPF190N60 | SiHA22N60AE |
| 27 | TPH3212PS | —— | —— | SiHP28N65E |
| 35 | TPH3205WSBQA | IPP65R099C6 | FCP125N65S3 | SiHG33N65EF |
| 47 | TP65H035WS | SPW47N65C3 | FCH47N60 | SiHW47N65E |

The FOM (figure of merit) of the device is the product of gate charge $Q_g$ and the conducting state resistance $R_{ds\_on}$ in normal operation. Generally, the FOM or the product of gate-drain charge $Q_{gd}$ of the device and the conducting resistance $R_{ds\_on}$ is used for measuring device performance. The smaller the product is, the better the device performance is.

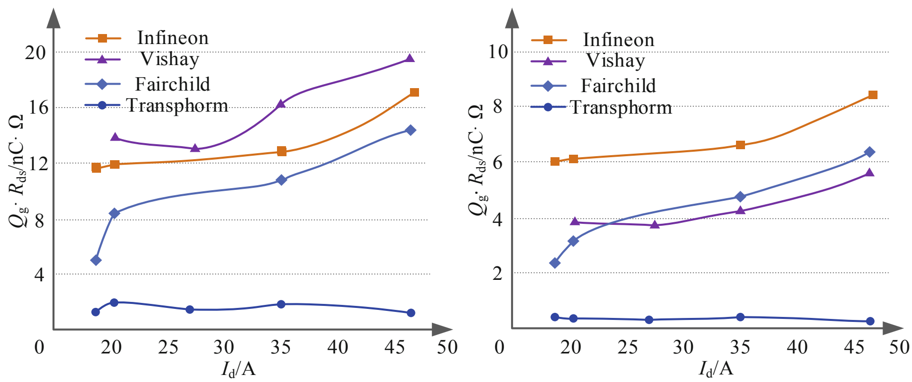


(a) FOM (b) $Q_{gd}R_{ds}$

**Fig. 1.** Performance comparison of devices.

With the continuous improvement of caspode GaN HEMT devices of Transphorm company and the introduction of improved models, the products are becoming more and more mature. At present, commercial products mainly include 650 V and 900 v series devices. Table 1 shows the selection of 650 V series devices of Transphorm with different current levels and Si MOSFETs with corresponding voltage and current levels from Infineon, Fairchild, and Vishay companies. Figure 1 shows the FOM value, gate-drain charge $Q_{gd,}$ and conducting resistance $R_{ds\_on}$ of the above devices. The product results are compared. It can be seen that the quality factor and $Q_{gd}R_{ds\_on}$ of GaN device are almost only 1/10 to 1/5 of that for Si MOSFET. And the performance gap becomes more and more evident with the increase of current. The results show that cascode GaN HEMT has better performance than Si MOSFET, and the higher the power level is, the more pronounced the advantage is.

## 2.2 Transfer Characteristics Analysis

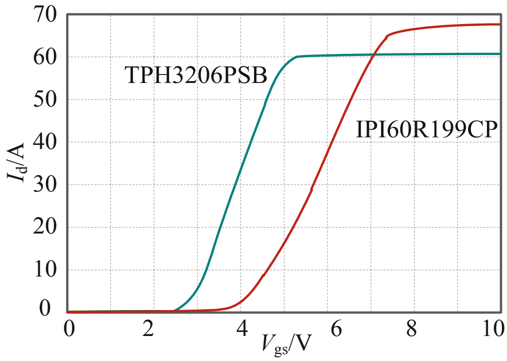


**Fig. 2.** Transfer characteristic curves comparison.

As a voltage-controlled current mode device, the transfer characteristic characterizes the ability of gate-source voltage $V_{gs}$ to amplify drain current $I_d$, and the slope of the transfer characteristic curve is transconductance $g_{fs}$. Figure 2 shows the comparison between TPH3206PSB and IPI60R199CP when $V_{ds} = 10$ V and temperature is 25 °C. It can be seen that the threshold voltage $V_{TH}$ of cascode GaN HEMT is lower than that of Si MOSFET. The typical threshold voltage of TPH3206PSB is 2.1 V, and that of IPI60R199CP is 3 V. Cascode GaN HEMTs have better voltage to current amplification ability than Si MOSFETs. In cascode structure, the turn-on and turn-off of depletion GaN HEMT is controlled by low voltage Si MOSFET of gate-source, which has little effect on the overall threshold of the device. The overall threshold of the apparatus mainly depends on the low voltage Si MOSFET of gate-source of GaN HEMT, while the threshold voltage of low voltage Si MOSFET is lower than that of high voltage Si MOSFET. Therefore, the threshold voltage of cascode GaN HEMT is lower than that of Si MOSFET with the same voltage level, and the gate-source voltage has a stronger amplification ability to drain current.

## 2.3 Driving Characteristic Analysis

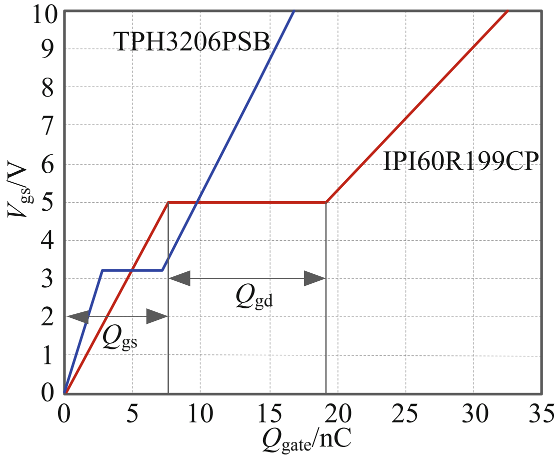


**Fig. 3.** Gate charge curves comparison.

The gate charge characteristic is the relation curve between the driving charge and the gate-source voltage of the device in the switching process. Because the switching time of the device in the circuit is related to the inter-electrode parasitic capacitance, and the inter-electrode parasitic capacitance is a function of the drain-source voltage VDS of the device, in order to facilitate the circuit design, in the actual application process, Generally, the switching speed is calculated. The driving circuit is designed by the gate charge characteristic curve of the device. Figure 3 shows the comparison of gate charge characteristic curves of TPH3206PSB and IPI60R199CP at $V_{ds} = 400$ V and $I_d = 10$ A. Taking the gate characteristic of IPI60R199CP as an example, $Q_{gs}$ is the charge required to charge the gate-source parasitic capacitor $C_{gs}$ to the threshold voltage, and $Q_{gd}$ is the charge required to overcome the "Miller effect" in the switching process of the device, also known as "Miller charge". It can be seen that the gate charge of GaN device is much less than that of Si MOSFET, significantly the Miller platform charge $Q_{gd}$ is only one-fifth of it. It ensures faster-driving speed, shorter switching time, and less loss of Gan devices under the same driving conditions.

**Table 2.** Contrast of driving characteristic related parameters.

| Device model | Driving voltage range/V | Threshold voltage/V | $Q_{gs}$/nC | $Q_{gd}$/nC | $Q_g$/nC |
|---|---|---|---|---|---|
| TPH3206PSB | ±18 | 2.1 | 2.1 | 2.2 | 6.2 |
| IPI60R199CP | ±20 | 3 | 8 | 11 | 32 |

Table 2 shows the parameters related to device driving. It can be seen that the driving voltage range of cascode GaN HEMT is similar to that of Si MOSFET. The Si MOSFET driver chip widely used at present can be directly used to drive cascode GaN HEMT, but the threshold voltage of the latter is lower than that of Si MOSFET, which is more likely to lead to misdirection of gate-source interference. Due to the high d*v*/d*t* and d*i*/d*t* in the switching process of Gan power devices, the switching process is more easily affected by parasitic parameters, which makes the coupling between the drive circuit and the power circuit become serious, and the voltage and current oscillation of the drive circuit may be intensified or turned on by mistake. Therefore, it is necessary to optimize the switching speed of GaN by selecting the appropriate driving resistor and optimizing the PCB layout of the primary power circuit and driving circuit to reduce the parasitic parameters.

At the same time, due to the existence of common-mode capacitor $C_{IO}$ in the drive isolator, the high d*v*/d*t* in the process of turning on the device will generate common-mode current in the front controller of the driver chip, and the larger the common mode capacitor $C_{IO}$ and d*v*/d*t*, the larger the common-mode current. Because the d*v*/d*t* of GaN devices is much higher than that of Si MOSFET, it is essential to select a suitable low common-mode capacitor driver. In response to this problem, a digital isolator can be added between the driver chip and the front-end controller, but this undoubtedly increases the complexity and cost of the driver. Therefore, the development and production of driver isolation chips with low common-mode capacitance is a better choice for the application of GaN devices in the future.

## 2.4 Comparison of Switch Characteristic Parameters

The switching characteristics of power devices are mainly related to the inter-electrode parasitic capacitance. The smaller the inter-electrode parasitic capacitance is, the shorter the charging time is, and the closer the switching process is to the ideal state. The inter-electrode parasitic capacitance of power devices mainly consists of gate-source parasitic capacitance $C_{gs}$, gate-drain parasitic capacitance $C_{gd}$, drain-source parasitic capacitance $C_{ds}$. In practical application, input capacitance $C_{iss}$, feedback capacitance $C_{rss}$ and output capacitance $C_{oss}$. Equation (1) is usually used to express the conversion relationship among them.

$$\begin{cases} C_{iss} = C_{gs} + C_{gd} \\ C_{rss} = C_{gd} \\ C_{oss} = C_{ds} + C_{gd} \end{cases} \quad (1)$$

Table 3 shows the comparison of switching characteristic parameters between TPH3206PSB and IPI60R199CP. The test conditions of TPH3206PSB are: $V_{gs} = 0\text{V}$, $V_{ds} = 400\text{V}, f = 1$ MHz. The test conditions of IPI60R199CP parameters are: $V_{gs} = 0$ V, $V_{ds} = 100$ V, $f = 1$ MHz (Generally speaking, the parasitic capacitance between electrodes is constant when $V_{ds}$ exceeds 100 v. therefore, the difference of $V_{ds}$ test conditions does not affect the comparison. It can be seen that the parasitic capacitance of cascode GaN HEMT is much smaller than that of Si MOSFET, which makes the switching characteristics better. Compared with Si MOSFET, the turn-on delay $t_{d(on)}$, turn-on gate-source voltage-rise time $t_r$, turn off delay $t_{d(off)}$, and turn off gate-source voltage drop time $t_f$ are greatly reduced so that the voltage and current intersection time in the switching process is reduced, and the switching loss is reduced, which provides the necessary conditions for greatly increasing the switching frequency of the converter.

**Table 3.** Switching characteristic related parameters comparison.

| Device model | $C_{iss}$/pF | $C$rss/pF | $C_{oss}$/pF | $t_d$(on)/ns | $t_r$/ns | $t_d$(off)/ns | $t_f$/ns |
|---|---|---|---|---|---|---|---|
| TPH3206PSB | 720 | 5.5 | 46 | 6 | 4.5 | 9.7 | 4 |
| IPI60R199CP | 1520 | —— | 72 | 10 | 5 | 50 | 5 |

Table 4 shows the reverse recovery characteristic parameters of TPH3206PSB and IPI60R199CP: peak reverse recovery current $I_{RP}$, reverse recovery time $t_{rr}$, reverse recovery charge $Q_{rr}$. Because the depletion type high voltage GaN HEMT in cascode GaN HEMT structure adopts two-dimensional electron gas conduction channel, there is no PN junction in Si based device and parasitic body diode, so there is no reverse recovery problem. At the same time, the breakdown voltage of Si MOSFET in cascode structure is lower, the reverse recovery characteristic of the parasitic diode is better than that of high voltage Si MOSFET, and the reverse recovery charge $Q_{rr}$ is much smaller. Therefore, the reverse recovery charge $Q_{rr}$ of cascode GaN HEMT is much smaller than that of Si MOSFET with the same voltage and current. It can be seen from Table 4 that the reverse recovery charge $Q_{rr}$ of TPH3206PSB is less than 1% of IPI60R199CP. In some bridge topologies, due to the sizeable reverse recovery charge of Si MOSFET, the current spike is often caused when the complementary transistor is turned on, so it is easy to damage the device. In order to solve this problem, the fast recovery diodes are paralleled in engineering applications. When Gan devices are used, the anti-parallel fast recovery diode can be omitted, and the stability of the converter can be improved.

**Table 4.** Comparison of parameters related to reverse recovery characteristics.

| Device model | $I_{RP}$/A | $t_{rr}$/ns | $Q_{rr}$/nC |
|---|---|---|---|
| TPH3206PSB | 10 | 17 | 52 |
| IPI60R199CP | 33 | 340 | 5500 |

### 2.5 Working Modal Analysis

According to the common-gate and common-source structure of cascode GaN HEMT, its different working modes are analyzed. In order to study its working principle under different working modes, the equivalent circuit model of cascode GaN HEMT is given in Fig. 4.

When the drain and source of the device are under forwarding voltage, the applied voltage is divided on different parasitic capacitors in the machine. When the gate-source

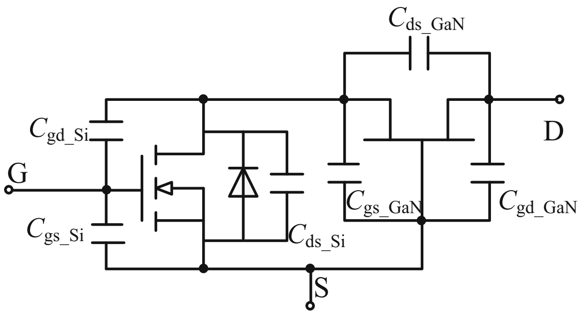


**Fig. 4.** Cascode GaN HEMT equivalent circuit.

driving voltage $V_{gs}$ of cascode GaN HEMT is less than the threshold voltage $V_{TH\_Si}$ of Si MOSFET, the Si MOSFET and depletion GaN HEMT are both in the off state, and there is no current flowing through the device, so the device is in the forward blocking state. When the gate-source driving voltage $V_{gs}$ is greater than the threshold voltage $V_{TH\_Si}$ of Si MOSFET, Si MOSFET starts to turn on, and its drain-source parasitic capacitance $C_{ds\_Si}$ begins to discharge due to the parallel with gate-source parasitic capacitance $C_{gs\_GaN}$ of depletion GaN HEMT and drain-source parasitic capacitance $C_{ds\_Si}$ of Si MOSFET. $C_{gs\_GaN}$ also starts to release the power, and the gate-source voltage $V_{gs\_GaN}$ of depletion GaN HEMT rises. The conduction channel is open, and the whole device is opened in the positive direction. The current flow in the device is shown in Fig. 5.

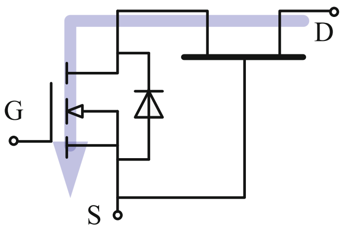


**Fig. 5.** Cascode GaN HEMT forward conduction mode.

When the drain and source of the device bear the reverse voltage, the device is in reverse conduction mode. Due to the existence of Si MOSFET parasitic diode, the current may flow through different conductive channels, resulting in an additional reverse conduction voltage drop of the device. The main problems are as follows:

(1) Si MOSFET body diode conduction: when the gate-source driving voltage $V_{gs}$ is less than the threshold voltage $V_{TH\_Si}$ of Si MOSFET, the bulk diode is on, and the channel is off. The current flows through the bulk diode of Si MOSFET, $i_{sd}$ is the reverse conduction current, $R_{ds\_GaN}$ is GaN HEMT conducting resistance, $V_{F\_Si}$ is the diode voltage drop of Si MOSFET, as shown in Fig. 6(a). At this time, the

reverse conduction voltage drop of cascode GaN HEMT is as follows.

$$V_{sd} = i_{sd} \cdot R_{ds\_GaN} + V_{F\_Si} \tag{2}$$

(2) Si MOSFET channel conduction: when the device gate-source driving voltage is large, the channel on state resistance $R_{ds\_Si}$ of Si MOSFET is small, and its source-drain voltage drop is less than the reverse conduction voltage drop of Si MOSFET body diode. The current flows through the channel of Si MOSFET, as shown in Fig. 6(b). In this case, the reverse conduction voltage drop of cascode GaN HEMT is as follows.

$$V_{sd} = i_{sd} \cdot (R_{ds\_Si} + R_{ds\_GaN}) \tag{3}$$

(3) Si MOSFET channel and body diode conduct simultaneously: when the device gate-source driving voltage is greater than the threshold voltage VTH_Si of Si MOSFET, the driving voltage is small, the channel conducting state resistance $R_{ds\_Si}$ of Si MOSFET would be significant. When the current flows through the track, the source and drain voltage drop may be greater than the reverse conduction voltage $V_{F\_Si}$ of Si MOSFET bulk diode. At this time, the parasitic diode of Si MOSFET is turned on, and its reverse conduction voltage is clamped at $V_{F\_Si}$. The current flows through the channel of Si MOSFET and the body diode at the same time, as shown in Fig. 6(c). The reverse conduction voltage drop of cascode GaN HEMT is as follows.

$$V_{sd} = i_{sd} \cdot R_{ds\_GaN} + V_{F\_Si} \tag{4}$$

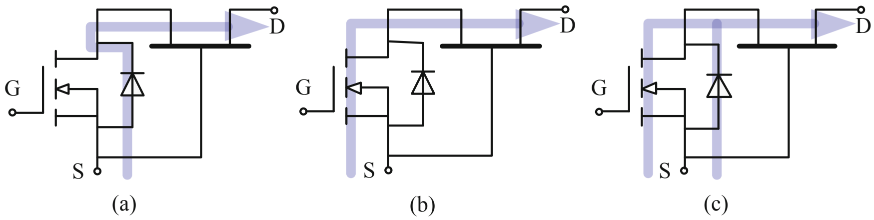


**Fig. 6.** Cascode GaN HEMT reverse conduction mode.

## 3 Experimental Verification

In order to verify the accuracy of the analytical model derived in this paper, the mathematical calculation software is used to solve the above analytical model of the switching process, and the voltage and current waveforms of the turn-on and turn-off process are made. The dual-pulse test platform is built and compared with the model results.

**Table 5.** Model verification experimental parameters.

| Parameter | Values | Unit |
|---|---|---|
| Input voltage $V_{in}$ | 450 | V |
| Drain parasitic inductance $L_D$ | 2 | nH |
| Source parasitic inductance $L_S$ | 1.5 | nH |
| Gate parasitic inductance $L_G$ | 2 | nH |
| Driving resistor $R_G$ | 15 | Ω |

Both $Q_L$ and $D_H$ are cascode GaN HEMT TPH3206PSB made by Transphorm company. The upper $D_H$ gate source is short-circuited and used as a freewheeling tube. The experimental parameters are shown in Table 5.

In the design of dual-pulse hardware platform, the value of parasitic inductance is not easy to control. Through the calculation of drive circuit and power circuit on PCB by Saturn PCB software, the parasitic inductance value of drive circuit $L_{Dri} = 3.2$nH, and the total parasitic inductance value of power circuit $L_{Pow} = 3.8$nH are obtained. It is basically consistent with the model validation parameters. The double pulse test platform is shown in Fig. 7. Figure 8 shows the experimental waveforms and switching process waveforms when $i_d$ is 10A.

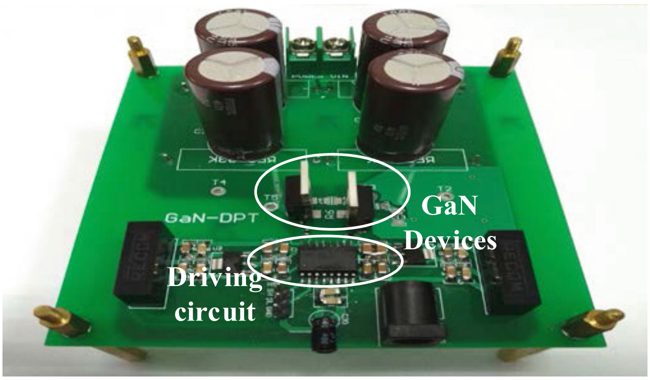


**Fig. 7.** Gallium nitride device dual-pulse test experimental platform.

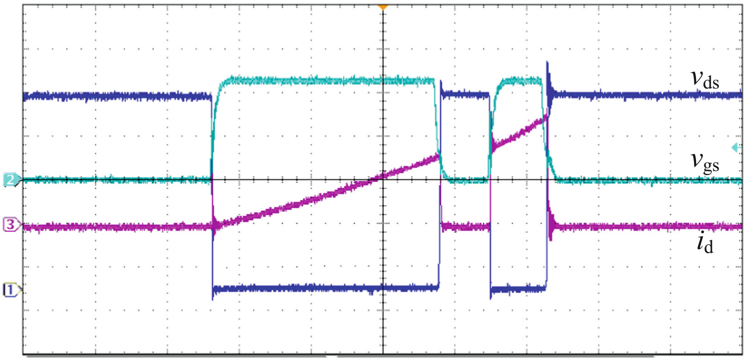


**Fig. 8.** Experimental waveforms of double pulse test.

## 4 Conclusions

In order to promote the substitution of cascode GaN HEMT for Si MOSFET, this chapter firstly compares the performance index of cascode GaN HEMT with Si MOSFET at the same voltage and current level. It makes clear that GaN device is superior to Si-based device. At the same time, the output characteristics, transfer characteristics, driving factors, and switching characteristics of cascode type GaN HEMT are compared with Si MOSFET at the same voltage and current level. The advantages of different attributes of cascode type GaN HEMT are explained. The reverse conduction voltage of cascode type GaN HEMT is slightly higher, and the size of common-mode capacitance should be paid attention to in driver selection. Finally, the different operation modes of cascode GaN HEMT are analyzed. In order to clarify the mechanism of the influence of various parameters on the switching process and obtain more accurate switching loss, an analytical model of cascode type GaN HEMT switching process is established in this chapter by reasonably segmenting and simplifying the switching process and considering the influence of reverse recovery of the complementary transistor. A double pulse test platform is built to verify the accuracy of the model. It is confirmed that the voltage and current waveforms in the switching process are more consistent with the measured waveforms, and the switching loss is more accurate.

**Acknowledgements.** The authors acknowledge the Jiangsu University Natural Science Research Project (18KJB470024) and Provincial Construction System Science and Technology Project of Jiangsu Provincial Housing and Urban-Rural Construction Department (2018ZD088). This work is partly supported by the Natural Science Foundation of Jiangsu Province of China (No. BK20161165), the applied fundamental research Foundation of Xuzhou of China (No. KC17072). The authorized patents for invention are also the research and development of Jiangsu Province Industry-University-Research Cooperation Project (BY2019056).

## References

1. Huang, X., Liu, Z., Qiang, L., Lee, F.C.: Evaluation and application of 600V GaN HEMT in cascode structure. In: 2013 Twenty-Eighth Annual IEEE Applied Power Electronics Conference and Exposition (APEC). IEEE (2013)
2. She, S., Zhang, W., Huang, X., Du, W., Qiang, L.: Thermal analysis and improvement of cascode GaN HEMT in stack-die structure. In: Energy Conversion Congress and Exposition. IEEE (2014)
3. Li, Y., Zhang, Y., Zheng, T.Q., Huang, B., Guo, X.: Research on output volt-ampere characteristics of cascode gan hemt and its application in single-phase inverter. Trans. China Electrotechnical Soc. (2015)
4. Chou, P.C., Cheng, S.: Performance characterization of gallium nitride HEMT cascode switch for power conditioning applications. Mater. Sci. Eng. B **198**, 43–50 (2015)
5. Sriram, S., Alcorn, T., Radulescu, F., Sheppard, S.: Cascode structures for GaN HEMTs. US20140361341 (2014)
6. Elangovan, S., Lin, J., Heng, C.S.: Reliability characterization of Gallium Nitride (GaN) HEMT cascode switch for power electronics applications. In: Sixteenth International Conference on Flow Dynamics (2020)
7. Green, B.M., Chu, K.K.: Cascode connected algan/gan hemts on sic substrates. IEEE Microwave Guided Wave Lett. **10**(8), 316–318 (2000)
8. Chou, P.-C., Chen, S.-H., Hsieh, T.-E., et al.: Evaluation and reliability assessment of GaN-on-Si MIS-HEMT for power switching applications. Energies (2017)
9. Liu, Z.: Characterization and failure mode analysis of cascode GaN HEMT. Virginia Tech (2014)
10. Ma, H., Zhang, N., Lin, L.Y.: Switching model of GaN HEMT in cascode configuration. J. Zhejiang Univ. (2016)
11. Chou, P.-C., Cheng, S.: Performance characterization of gallium nitride HEMT cascode switch for power conditioning applications. Mater. Sci. Eng. B. Solid-State Mater. Adv. Technol. (2015)
12. Sriram, S.: Cascode structures for GaN HEMTs (2017)
13. Swain, R., Jena, K., Lenka, T.R.: Modelling of capacitance and threshold voltage for ultrathin normally-off algan/gan moshemt. Pramana - J. Phys. **88**, 3 (2017). https://doi.org/10.1007/s12043-016-1310-y
14. Liu, Z., Huang, X., Zhang, W., Lee, F.C., Li, Q.: Evaluation of high-voltage cascode GaN HEMT in different packages. In: IEEE Applied Power Electronics Conference and Exposition-APEC, pp.168–173. IEEE (2014)
15. Zhang, W., Xu, Z., Zhang, Z., Wang, F., Blalock, B.J.: Evaluation of 600 V cascode GaN HEMT in device characterization and all-GaN-based LLC resonant converter. In: Energy Conversion Congress and Exposition. IEEE (2013)
16. Huang, X., Liu, Z., Qiang, L., Lee, F.C.: Evaluation and application of 600V GaN HEMT in cascode structure. APEC (2013)
17. Cheng, S., Chou, P.C.: Power conditioning applications of 700V GaN-HEMTs cascode switch. in: Conference of the IEEE Industrial Electronics Society. IEEE (2016)